

all the parameters is included, the total change ΔQ_e for $s=0$, $\gamma=1$ is predicted to be

$$\begin{aligned}\Delta Q_e &= -(2.2 - 90\Delta C_3/C_3 \pm 1.6) \mu V/^\circ K & (280^\circ K) \\ &= -(2.9 - 140\Delta C_3/C_3 \pm 1.7) \mu V/^\circ K & (240^\circ K) \\ &= -(13.8 - 410\Delta C_3/C_3 \pm 3.6) \mu V/^\circ K & (120^\circ K). \quad (3)\end{aligned}$$

The indicated uncertainty is largely due to the fact that the pressure dependences of the effective masses have not been measured directly as yet. This uncertainty and the experimental uncertainty are large enough so that it is not possible at present to limit the ranges of s and γ , the choice $s=0$, $\gamma=1$ just being used as an example, but it can be said that $|\Delta C_3/C_3| \lesssim 0.01$, which is about the same as $\Delta C_2/C_2$, and reasonable. There is very little difference between Eq. (3) and the

results when only C_2 is considered, because the other pressure changes tend to cancel each other; if they were all of the same sign, the predictions would differ by about 100%.

Similar conclusions result from the analysis of p -type germanium, but here the treatment is complicated by the presence of two bands of holes that contribute to the thermoelectric power. The dependence upon C_2 , however, is unchanged, and again this is the most important single term. When the analysis is made including all parameters by determining mass changes from the $\mathbf{k} \cdot \mathbf{p}$ method, it is found that for $s=0$, $\gamma=1$,

$$\begin{aligned}\Delta Q_h &= (1.3 - 100\Delta C_3/C_3 \pm 0.6) \mu V/^\circ K & (280^\circ K) \\ &= (2.1 - 150\Delta C_3/C_3 \pm 0.8) \mu V/^\circ K & (240^\circ K) \\ &= (11.4 - 780\Delta C_3/C_3 \pm 2.3) \mu V/^\circ K & (120^\circ K). \quad (4)\end{aligned}$$

Interband Magnetoabsorption in InAs and InSb

C. R. PIDGEON

National Magnet Laboratory, Massachusetts Institute of Technology, Cambridge, Massachusetts*

AND

D. L. MITCHELL

U. S. Naval Research Laboratory, Washington, D. C.

AND

R. N. BROWN†

National Magnet Laboratory, Massachusetts Institute of Technology, Cambridge, Massachusetts*

(Received 1 August 1966)

Direct interband magneto-optical transitions have been observed in bulk and epitaxial films of InAs with magnetic fields up to 100 kOe. The results are interpreted using a modification of the method of Luttinger and Kohn which includes the effects of nonparabolic conduction and light-hole bands, and warping of the conduction and valence bands. The following band parameters at $\mathbf{k}=0$ are obtained for $T \sim 20^\circ K$: conduction-band effective mass $m_c = 0.0240m_0$; light-hole effective mass $m_{lh} = 0.026m_0$; and conduction-band g factor $g_c = -15$. Further experimental results (obtained from magnetoabsorption data) are given for the energy dependence of the conduction-band g factors in InSb and InAs. These are compared with the results computed theoretically.

INTRODUCTION

ALTHOUGH the main features of the one-electron energy-band structure of InAs are well known, the set of band parameters which describe this band structure are not well determined (for example, see Madelung¹). The interband magnetoabsorption experiment is particularly useful for this purpose, since it allows the valence and conduction bands to be accurately probed with polarized radiation over an

extended energy range. A set of measurements on a single sample (at selected orientations) is sufficient to determine the full set of band parameters which describe the conduction band and the three valence bands in the vicinity of the Γ point of the Brillouin zone ($\mathbf{k}=0$). Zwerdling *et al.*² performed magnetoabsorption measurements on InAs at room temperature but only observed the first two broad transmission minima. Recently, Johnson³ has obtained more detailed spectra at 1.5 and 77°K with magnetic fields up to 20 kOe. In the present work the direct interband

* Supported by the U. S. Air Force Office of Scientific Research.
† Present address: Schlumberger Well Surveying Corporation, Ridgefield, Connecticut.

¹ O. Madelung, *Physics of III-V Compounds*, translated by D. Meyerhofer (John Wiley & Sons, Inc., New York, 1964), pp. 23, 349.

² S. Zwerdling, B. Lax, and L. M. Roth, *Phys. Rev.* **108**, 1402 (1957).

³ E. Johnson, Ph.D. dissertation, Purdue University, 1964 (unpublished).

magnetoabsorption was investigated in bulk InAs at approximately 20°K and in epitaxial InAs⁴ at 4.2, 77, and 300°K. Magnetic fields up to 100 kOe were used and the effects of band nonparabolicity were clearly observed.

The theory of interband magneto-optical phenomena for semiconductors of the Ge type has been given by various authors (Elliott *et al.*,⁵ Roth *et al.*,⁶ and Burstein *et al.*⁷) using the effective-mass method of Luttinger and Kohn⁸ (LK). However, in the case of small-band-gap semiconductors (such as InSb and InAs) it is well known that it is not sufficiently accurate to treat the conduction-valence-band interaction by perturbation theory, as has been shown in detail for the zero-field case by Kane.⁹ Several authors have extended the approach of Kane to the case of an applied magnetic field (see, for example, Bowers and Yafet¹⁰). In a previous paper (Pidgeon and Brown¹¹ hereafter referred to as I) the magnetic energy levels in the valence and conduction bands of InSb were calculated by a method which includes the effect of higher bands to order k^2 in effective-mass theory. The resulting interaction between the three valence bands and the conduction band was then solved exactly. Measurements of the interband magnetoabsorption were interpreted in terms of this model and a set of band parameters obtained for a good over-all fit of the spectra. In the present paper we use this method to interpret similar measurements on InAs. The magnetic energy levels in the valence and conduction bands at the zone center are computed as the solutions of two 4×4 numerical matrices for a given set of band parameters. The theoretical and experimental spectra for the principal allowed transitions are then compared and the band parameters successively adjusted to give the best over-all fit. The band-edge effective masses were calculated in terms of these parameters for the light-hole band and the conduction band.

Further experimental measurements are given for the energy dependence of the conduction band g factor in InSb and the band-edge g value in InAs. These are compared with the results computed theoretically.

THEORY

We briefly summarize the method given in detail in I. The magnetic energy levels are obtained according to

⁴ The epitaxial samples were kindly supplied by Texas Instruments, Inc.

⁵ R. J. Elliott, T. P. McLean, and G. C. MacFarlane, Proc. Phys. Soc. (London) **72**, 553 (1958).

⁶ L. M. Roth, B. Lax, and S. Zwerdling, Phys. Rev. **114**, 90 (1959).

⁷ E. Burstein, G. S. Picus, R. F. Wallis, and F. Blatt, Phys. Rev. **113**, 15 (1959).

⁸ J. M. Luttinger and W. Kohn, Phys. Rev. **97**, 869 (1955); J. M. Luttinger, *ibid.* **102**, 1030 (1956).

⁹ E. O. Kane, J. Phys. Chem. Solids **1**, 249 (1957).

¹⁰ R. Bowers and Y. Yafet, Phys. Rev. **115**, 1165 (1959); Y. Yafet, *ibid.* **115**, 1172 (1959).

¹¹ C. R. Pidgeon and R. N. Brown, Phys. Rev. **146**, 575 (1966).

the LK model with the modification that the conduction band is treated together with the degenerate valence-band set. The following set of coupled equations is obtained (in atomic units) for the eigenvalues and eigenvectors of the system:

$$\sum_{j'} \left\{ D_{jj'}^{\alpha\beta} k_{\alpha} k_{\beta} + \pi_{jj'}^{\alpha} k_{\alpha} + \frac{s}{2} (\sigma_3)_{jj'} + \frac{1}{4c^2} [(\boldsymbol{\sigma} \times \nabla V) \cdot \mathbf{p}]_{jj'} + \epsilon_{j'} \delta_{jj'} \right\} f_{j'}(\mathbf{r}) = \epsilon f_j(\mathbf{r}), \quad (1)$$

where the notation is defined in I. The functions $f_j(\mathbf{r})$ are the usual envelope functions where j and j' run over the two conduction and six valence-band states. Taken in order term 1 in Eq. (1) represents the interaction with higher bands included to order k^2 in effective-mass theory. Term 2 gives the direct interaction between conduction and valence bands which reduces to the $\mathbf{k} \cdot \mathbf{p}$ interaction term⁹ in zero magnetic field. Term 3 gives the free-electron spin magnetic energy (s is proportional to the magnetic field \mathbf{H}) and term 4 is the momentum(\mathbf{p})-dependent part of the spin-orbit interaction which is diagonalized in the J, m_j representation of the effective-mass matrix.

The effective-mass Hamiltonian is written as an 8×8 matrix D in the J, m_j representation. Following Luttinger,⁸ it is assumed that \mathbf{H} is in the $(1\bar{1}0)$ plane, and D is written in two parts

$$D = D_0 + D_1, \quad (2)$$

where the principal anisotropy is included in D_0 which is treated exactly. The other part in D_1 may be treated by perturbation theory. D_0 is given in terms of two 4×4 numerical matrices D_a and D_b , by

$$D_0 = \begin{pmatrix} D_a & 0 \\ 0 & D_b \end{pmatrix}. \quad (3)$$

This gives two eigenvalue equations that are solved exactly for a given set of band parameters. We have here made the approximation that $k_H = 0$, and neglected certain small higher band terms. The four solutions to the a matrix represent the conduction, heavy-hole, light-hole, and split-off bands, respectively; the four solutions to the b matrix give the corresponding states of opposite spin.

Included in this approach are the nonparabolic effects of conduction and valence bands resulting from the direct $\mathbf{k} \cdot \mathbf{p}$ interaction, and the warping and "quantum" effects⁸ in the light- and heavy-hole valence bands resulting from the higher band interactions. In addition, by solving Eq. (3) exactly, we include the warping effects of higher bands on the conduction band, i.e., anisotropy in the conduction band can only arise from terms of order k^4 and higher, and these are effectively generated by this diagonalization procedure. This gives

a small anisotropy of the conduction-band effective mass, but a larger anisotropy of the corresponding effective g factor. These conduction-band effects have recently been discussed in detail for InSb using a perturbation method by Ogg.¹² The anisotropy of the conduction band has also been considered by Bell and Rogers.¹³ Numerical results obtained from the computations of the present work are given in the final section of this paper.

EXPERIMENTAL METHOD

Conventional techniques were used for measuring magnetoabsorption spectra of bulk and epitaxial films of InAs. Bulk samples of about $5\text{-}\mu$ thickness were mounted on sapphire discs in a copper "heat sink" arrangement. In this case, the sample temperature was estimated to be about 20°K . Confirmatory magneto-reflection measurements were also made on thick bulk samples to look for possible strain effects resulting from gluing to a sapphire substrate. In fact, the expansion coefficients of InAs and sapphire match quite well, and no strain effects (line splittings or shifts) were observed to within the accuracy of the experiment. The epitaxial films (of thickness between 4 and $8\ \mu$) were deposited on GaAs substrates. Measurements were performed on these samples immersed in the coolant at liquid-helium, nitrogen, and room temperatures. The mobilities were somewhat higher than those of the bulk samples. The majority of the measurements were done on a sample with a carrier concentration of the order $1 \times 10^{16}\ \text{cm}^{-3}$. Strain effects should be completely negligible. The thermal expansion coefficients of InAs and GaAs are closely matched over a temperature range from nitrogen temperature to well above room temperature.¹⁴ The strain shift of the energy gap at 4.2°K was conservatively calculated to be less than $1\ \text{meV}$ and any strain splittings would be correspondingly smaller.

EXPERIMENTAL RESULTS

Bulk Samples

In Fig. 1 are shown plots of photon energy of the observed transmission minima as a function of magnetic field strength for transitions in the $\mathbf{E} \perp \mathbf{H}$ (i.e., σ_L and σ_R) spectrum. Unfortunately, the expected fine structure was not resolved in detail, so that the theoretical assignment had to be made in terms of only the *principal* allowed transitions. Because of this it was not possible to measure the small anisotropy of the spectra

¹² N. Ogg, Proc. Phys. Soc. (London) **89**, 431 (1966). A small anisotropy of the conduction-band effective mass has been observed by G. A. Antcliffe and R. A. Stradling [Phys. Letters **20**, 119 (1966)] in de Haas-Shubnikov measurements.

¹³ R. L. Bell and K. T. Rogers, Interim Report No. 9, Varian Associates, 1964 (unpublished); Central Research Memorandum 188, 1966 (unpublished).

¹⁴ N. N. Sirota and Yu. I. Pashinzev, Dokl. Akad. Nauk SSSR **127**, 609 (1959).

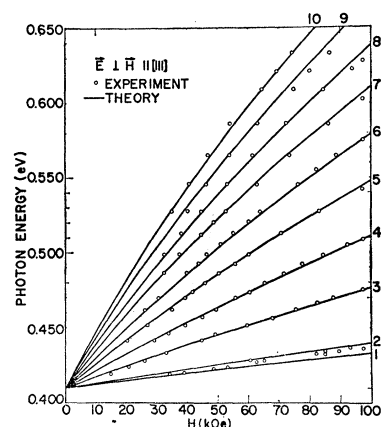


FIG. 1. Plot of the photon energy of the principal transmission minima as a function of magnetic field for $\mathbf{E} \perp \mathbf{H}$. The notation for the transitions is defined in I. The solid lines are obtained from Eqs. (17) and (18) in I. The transitions are as follows:

- | | |
|-------------------|--------------------|
| 1. $a^-(2)a^c(0)$ | 6. $b^+(2)b^c(2)$ |
| 2. $b^+(0)b^c(0)$ | 7. $a^+(4)a^c(2)$ |
| 3. $a^+(2)a^c(0)$ | 8. $b^+(3)b^c(3)$ |
| 4. $b^+(1)b^c(1)$ | 9. $a^+(5)a^c(3)$ |
| 5. $a^+(3)a^c(1)$ | 10. $b^+(4)b^c(4)$ |

(observed in I for InSb). In Fig. 2 are shown similar plots for the $\mathbf{E} \parallel \mathbf{H}(\pi)$ spectrum, again with the strongest allowed transitions associated with the observed transition minima. The nonparabolic effects of conduction and valence bands are clearly shown by the curvature of the lines.

A plot of the ratio of radiation intensity transmitted with a magnetic field applied to that at zero field, $I(H)/I(0)$, as a function of photon energy is shown in Fig. 3 for the Faraday (σ) configuration $\mathbf{E} \perp \mathbf{H}$ at $97.5\ \text{kOe}$.

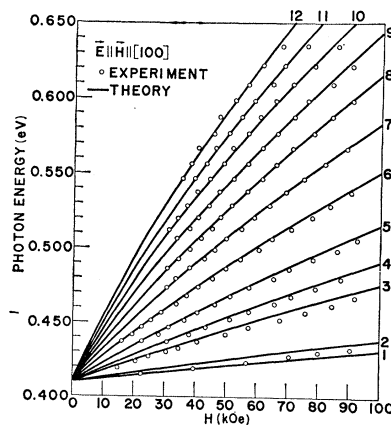


FIG. 2. Plot of the photon energy of the principal transmission minima as a function of magnetic field for $\mathbf{E} \parallel \mathbf{H}$. The solid lines are obtained as in Fig. 1. The transitions are as follows:

- | | |
|-------------------|---------------------|
| 1. $b^-(2)a^c(0)$ | 7. $b^-(6)a^c(4)$ |
| 2. $a^+(0)b^c(0)$ | 8. $b^-(7)a^c(5)$ |
| 3. $b^-(3)a^c(1)$ | 9. $b^-(8)a^c(6)$ |
| 4. $a^+(1)b^c(1)$ | 10. $b^-(9)a^c(7)$ |
| 5. $b^-(4)a^c(2)$ | 11. $b^-(10)a^c(8)$ |
| 6. $b^-(5)a^c(3)$ | 12. $b^-(11)a^c(9)$ |

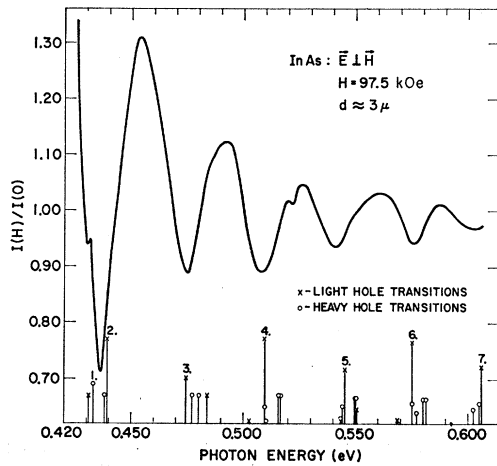


FIG. 3. Plot of the ratio of transmitted intensity with the magnetic field applied to that at zero field, $I(H)/I(0)$, against photon energy for $\mathbf{E} \perp \mathbf{H}$. The theoretical positions and relative strengths of the allowed ($\Delta n=0, -2$) transitions are shown beneath the spectra. Crosses represent light-hole transitions, circles represent heavy-hole transitions. The numbering 1 to 10 corresponds to the transitions shown in Fig. 1.

Epitaxial Films

In Fig. 4, typical plots are shown of $I(H)/I(0)$ vs photon energy for the purest epitaxial film in both the π and σ polarizations (at 99.6 kOe and 77°K). It is seen that somewhat more structure is observed in the spectra than in the case of bulk material, presumably because of the greater sample purity. However, there is also an over-all shift to higher energy of the principal transmission minima (~ 10 meV for $H=100$ kOe at 4.2°K) with respect to the equivalent bulk material spectra.

The low-temperature energy gaps for this sample (0.420 ± 0.003 eV at 4.2°K and 0.414 ± 0.003 eV at 77°K) are also 10–15 meV higher than those obtained by

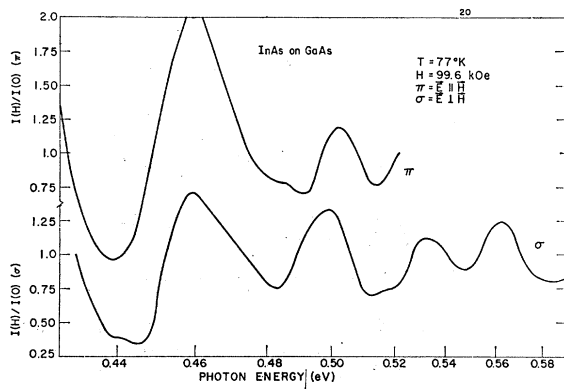


FIG. 4. Plots of $I(H)/I(0)$ against photon energy showing typical spectra for epitaxial films of InAs on GaAs at 77°K for $\mathbf{E} \parallel \mathbf{H}$ and $\mathbf{E} \perp \mathbf{H}$. The spin splitting of the first main line is clearly resolved. The splitting was verified by sweeping the magnetic field at fixed photon energies.

Johnson³ at these temperatures, while the room-temperature value (0.359 ± 0.003 eV) is in good agreement with the value (0.360 ± 0.002 eV) quoted by Zwerdling *et al.*² The origin of the discrepancy for the low-temperature values is not clear. Differential strain between film and substrate can account for only 1 meV of this difference, at most. It is possible that impurity effects account for part of the difference. Johnson³ observed a 4-meV increase in the energy gap, at both 1.5 and 77°K, when the carrier concentration was lowered from 5.3×10^{16} cm⁻³ to 2.0×10^{16} cm⁻³. The epitaxial sample had a still lower carrier concentration; however, it is not expected that this would account for the entire difference. We choose the low-temperature energy gap of the bulk sample for fitting the band parameters since it agrees with previous work³ and is less subject to uncertainty.

NUMERICAL RESULTS AND DISCUSSION

Band Parameters of InAs

We use the procedure discussed in I, taking existing cyclotron-resonance results (see Palik and Stevenson¹⁵) to obtain a preliminary set of parameters for the assignment of the principal transitions. Unfortunately, it was not possible to measure the anisotropy of the spectra, so we make the approximation of spherical symmetry, i.e., $\gamma_2^L = \gamma_3^L = \tilde{\gamma}^L$ in the notation of I. In addition, interband magnetoabsorption measurements are very insensitive to the heavy-hole mass, so we assume that this is the same as for InSb (i.e., $m_{h.h.} = 0.4 m_0$). This is a reasonable approximation since this mass is determined almost entirely by higher bands which are about as far away in energy for both cases. The energy gap ϵ_g is obtained from our experiments as 0.41 eV. We then obtain the following final set of band-edge parameters for a good over-all fit of the spectra:

$$P^2 = 0.38 \text{ atomic units (a.u.)},$$

$$\epsilon_g = 0.41 \text{ eV},$$

$$\Delta = 0.44 \text{ eV},$$

$$\gamma_1^L = 20.5,$$

$$\tilde{\gamma}^L = 9.0,$$

$$\kappa^L = 8.0.$$

Using these parameters, the solid lines obtained from the theory of I are shown in Figs. 1 and 2 for the principal light and heavy-hole transitions. In Fig. 3 we show the relative strengths and positions of all the ($\Delta n=0, -2$) allowed transitions for the σ spectrum.

Conduction-Band g Factor and Effective Mass in InSb and InAs

In the present work we have followed the approach of I by fitting the Landau level theory to transitions

¹⁵ E. D. Palik and J. R. Stevenson, Phys. Rev. **130**, 1344 (1963).

between the higher quantum-number levels where exciton effects should be unimportant (see Elliott and Loudon¹⁶). Exciton and impurity effects may be important in determining the absolute energies of the lowest transitions, but we assume in this section that the *difference* between the energies of adjacent transitions is approximately independent of these effects, at least for quantum numbers $n=1$ and upwards. We may then define a magnetic-field-dependent effective mass for the conduction band by

$$m_c^*(n, H) = eH/c(\epsilon_{n+1}^c - \epsilon_n^c). \quad (4)$$

This is the mass that is measured in cyclotron resonance. Similarly, we define an effective g factor (measured in spin resonance) by

$$g_c^*(n, H) = [eH/2c(\epsilon_{a,n}^c - \epsilon_{b,n}^c)]^{-1}. \quad (5)$$

It should be recognized, however, that the spin resonance may be excited by electric dipole radiation, in narrow-gap semiconductors such as InAs and InSb. This "combination" resonance, which is induced by the nonparabolicity, has been treated by Sheka¹⁷ for the case of InSb. The effective mass and g factor defined in (4) and (5) of course represent average values obtained over the energy increments $\Delta\epsilon_{an, a(n+1)}$ and $\Delta\epsilon_{an, bn}$, respectively, so that in the nonparabolic region of the band one must maintain the condition $\Delta\epsilon \ll \epsilon_n^c$ in order to obtain a true determination of the energy dependence of effective mass and g factor. It is not possible directly to relate the quantities defined in Eqs. (4) and (5) to the corresponding quantities measured in transport experiments since one cannot obtain an explicit expression for $\epsilon(n, H)$ or for $\epsilon(\mathbf{k})$ in this approximation. It is possible, however, to make meaningful comparisons under conditions of strict degeneracy and low magnetic fields. A detailed discussion of the relationship between effective masses determined by cyclotron resonance and those determined by Faraday rotation has been given by Palik *et al.*,¹⁸ in the approximation where higher band interactions are neglected and the interaction between conduction and valence bands is included only to 4th power of \mathbf{k} in effective-mass theory. The band-population contributions to the interband Faraday rotation can also give rise to apparent differences between the cyclotron mass and the corresponding mass obtained from measurement of the free-carrier Faraday rotation.¹⁹ These contributions, if not treated properly, lead to an apparent increase in the Faraday mass for conditions appropriate to n -type InSb and InAs.

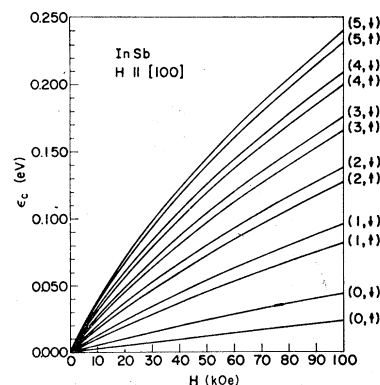
¹⁶ R. J. Elliott and R. Loudon, *J. Phys. Chem. Solids* **15**, 196 (1960).

¹⁷ V. I. Sheka, *Fiz. Tver. Tela* **6**, 3099 (1964) [English transl.: *Soviet Phys.—Solid State* **6**, 2470 (1965)].

¹⁸ E. D. Palik, G. S. Picus, S. Teitler, and R. F. Wallis, *Phys. Rev.* **122**, 475 (1961).

¹⁹ D. L. Mitchell, E. D. Palik, and R. F. Wallis, *Phys. Rev. Letters* **14**, 827 (1965).

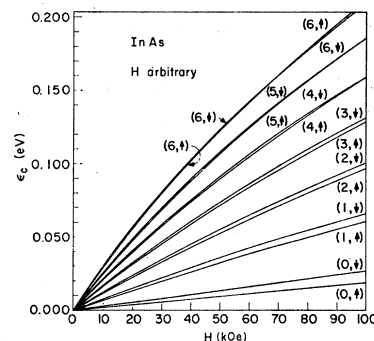
FIG. 5. Computed conduction-band energy levels for InSb as a function of magnetic field. The numbers in brackets are the Landau quantum number n for the levels and the arrows represent spin up (\uparrow) and spin down (\downarrow).



Theoretical computed curves for the energies of conduction-band levels versus H are shown in Fig. 5 for InSb (obtained from the results of I) and in Fig. 6 for InAs. From these we may calculate $m_c^*(n, H)$ and $g_c^*(n, H)$.

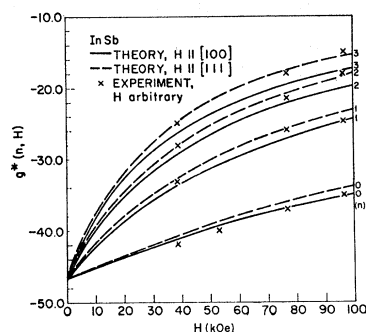
Computed results for $g_c^*(n, H)$ are shown in Figs. 7 and 8 for InSb and InAs, respectively. Two features

FIG. 6. Computed conduction-band energy levels for InAs as a function of magnetic field. The notation is the same as in Fig. 5. Note that for the $n=5$ levels the spin splitting goes to zero at about $H=100$ kOe, and that the $n=6$ levels cross over at about 75 kOe, implying a change of sign of the g factor.



resulting from higher band interactions are of interest. Firstly, in the case of InSb (where spherical symmetry has *not* been assumed) it is found that $g_c^*(n, H)$ is about 10 times as anisotropic as $m_c^*(n, H)$. For example, $g_c^*(n, H)$ for the $n=3$ Landau level at $H=88$ kOe along the $[100]$ direction is greater than that for \mathbf{H} along the $[111]$ direction by about 10%, whereas the corresponding effective masses differ by only about 1%

FIG. 7. Plots of the effective g factor, defined in Eq. (5), as a function of magnetic field for InSb. The crosses represent the experimental points and the lines represent the theoretical curves obtained as described in the text for $\mathbf{H} \parallel [100]$ and $[111]$. The numbers give the quantum number n .



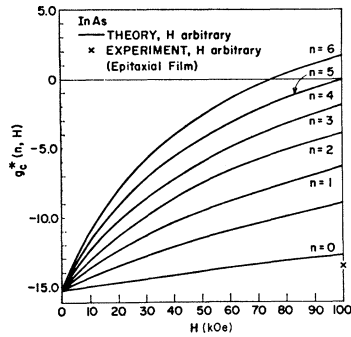


FIG. 8. Plots of $g_c^*(n, H)$ as a function of magnetic field for InAs for an arbitrary direction of H . The notation is the same as in Fig. 7.

(with the anisotropy going the opposite way). Secondly, in the case of InAs it is found that the magnitude of $g_c^*(n, H)$ decreases more rapidly with energy becoming zero, for example at $\epsilon_c \sim 0.18$ eV for $n=5$, and then becoming positive as ϵ_c increases. The first result for the ratio of anisotropies is in good agreement with that predicted by Ogg,¹² although there is a discrepancy in the absolute values obtained. This may be associated with different values of the higher band parameters assumed. The energy dependence of the g factor has been considered by Bowers and Yafet¹⁰ and by Zawadzki.²⁰ The change of sign of $g_c^*(n, H)$ in InAs at relatively low energies shows the modifying effects of higher bands on the prediction of Zawadzki, who showed from an extension of Roth's⁶ expression for the band edge g factor (which does not include the effects of higher bands) that *in this approximation* $g_c(\epsilon)$ goes to zero at $\epsilon \sim 0.65$ eV, finally tending to the free electron value of $+2$ at high ϵ .

For the case of InSb, where almost all the allowed transitions were clearly resolved in magneto-absorption spectra, it has been possible to determine $g_c^*(n, H)$ experimentally. Pairs of heavy hole \rightarrow electron transitions, separated essentially by the conduction-band g factor spin splitting were resolved up to high energy in both π and σ_R (i.e., right circularly polarized) spectra. From this we obtain $g_c^*(n, H)$ after subtracting off the small additional energy resulting from the difference in the heavy-hole levels involved. The experimental points obtained for an arbitrary direction of magnetic field are shown in Fig. 7. Unfortunately, it was not possible to resolve these spin splittings in the InAs spectra, except for the first principal transmission minimum of the σ spectra which was resolved in the

²⁰ W. Zawadzki, Phys. Letters 4, 190 (1963); Phys. Status Solidi 3, 1421 (1963).

epitaxial films (Fig. 4). This splitting was observed in magnetic field sweeps as well as in wavelength sweeps. The approximate band-edge value of $g_c^*(n, H)$ obtained from this is shown in Fig. 8.

CONCLUSIONS

Values for the low-temperature-band parameters ($P^2=0.38$ a.u., $E_g=0.41$ eV, $\Delta=0.44$ eV, $\gamma_1^L=20.5$, $\tilde{\gamma}^L=9.0$ and $\kappa^L=8.0$) were obtained by fitting to the observed magnetoabsorption transitions, assuming spherical symmetry and that the heavy-hole mass is the same as for InSb ($m_{h,h}=0.40 m_0$). Using these values, we deduce the following values of effective mass at $\mathbf{k}=0$ for $T \sim 20^\circ\text{K}$: $m_c=(0.024 \pm 0.001)m_0$; $m_{1,h}=(0.026 \pm 0.002)m_0$; and the conduction band g factor $g_c=(-15.0 \pm 1.0)$. The values for $m_{1,h}$ and $m_{h,h}$ are given by the expressions in the classical (large n) limit, $m_{1,h}=[1/(\gamma_1^L+2\tilde{\gamma}^L)]$, $m_{h,h}=[1/(\gamma_1^L-2\tilde{\gamma}^L)]$, which include the effects of higher bands. However, the values m_c and g_c were obtained from the expressions due to Kane⁹ and Roth,⁶ respectively.

Using the procedure described previously and extrapolating to low values of H (i.e., the parabolic region of the band) we obtain the following values for effective mass and g factor at $\mathbf{k}=0$: $\tilde{m}_c=0.0240 m_0$ and $\tilde{g}_c=-15$. These results are in good agreement with the cyclotron-resonance measurements of Palik and Stevenson.¹⁵ The value for \tilde{m}_c is about 8% lower than that obtained in Faraday rotation measurements at 77°K by Palik *et al.*,²¹ and more recently by Summers²² for samples with $N \sim 3 \times 10^{16} \text{ cm}^{-3}$. One source for such a discrepancy is associated with the distribution effect, which increases the apparent effective mass as measured by Faraday rotation where the conditions are not strictly degenerate. Another possible source is the band-population effects discussed previously.

ACKNOWLEDGMENTS

We wish to acknowledge Professor B. Lax for his support of this work, N. Ogg and R. A. Stradling for correspondence concerning the higher band effects on the conduction band of InSb, and S. Groves and W. Zawadzki for helpful discussions. We are grateful to J. Casteris for help with the construction of the apparatus.

²¹ E. D. Palik, S. Teitler, and R. F. Wallis, J. Appl. Phys. Suppl. 32, 2132 (1961).

²² C. J. Summers, Ph.D. thesis, Reading University, 1966 (unpublished).